

# Dipolar condensed atomic mixtures and miscibility under rotation

Lauro Tomio<sup>1\*</sup>, R. K. Kumar<sup>1,2</sup> and A. Gammal<sup>3</sup>

<sup>1</sup> Instituto de Física Teórica, Universidade Estadual Paulista, 01140-070 São Paulo, SP, Brazil.

<sup>2</sup> Department of Physics, Centre for Quantum Science, and Dodd-Walls Centre for Photonic and Quantum Technologies, University of Otago, Dunedin 9054, New Zealand.

<sup>3</sup> Instituto de Física, Universidade de São Paulo, 05508-090 São Paulo, Brazil.

\* lauro.tomio@gmail.com

November 6, 2019



*Proceedings for the 24th edition of European Few Body Conference,  
Surrey, UK, 2-4 September 2019*

1

## 2 Abstract

3 By considering symmetric and asymmetric dipolar coupled mixtures (with dysprosium  
4 and erbium isotopes), we report a study on relevant anisotropic effects, related to spa-  
5 tial separation and miscibility, due to dipole-dipole interactions (DDIs) in rotating binary  
6 dipolar Bose-Einstein condensates. The binary mixtures are kept in strong pancake-like  
7 traps, with repulsive two-body interactions modeled by an effective two-dimensional  
8 (2D) coupled Gross-Pitaevskii equation. The DDI are tuned from repulsive to attrac-  
9 tive by varying the dipole polarization angle. A clear spatial separation is verified in  
10 the densities for attractive DDIs, being angular for symmetric mixtures and radial for  
11 asymmetric ones. Also relevant is the mass-imbalance sensibility observed by the vortex-  
12 patterns in symmetric and asymmetric-dipolar mixtures. In an extension of this study,  
13 here we show how the rotational properties and spatial separation of these dipolar mix-  
14 ture are affected by a quartic term added to the harmonic trap of one of the components.

15

## 16 Contents

17	<b>1 Dipolar Bose-Einstein condensate - Introduction</b>	<b>2</b>
18	<b>2 Model formalism, parametrization and numerical approach</b>	<b>3</b>
19	2.1 Model formalism	3
20	2.2 Parametrization and numerical approach	4
21	<b>3 Symmetric and asymmetric dipolar mixtures - Results</b>	<b>4</b>
22	3.1 Dipolar mixtures confined by identical harmonic pancake-like traps	4
23	3.2 Dipolar symmetric $^{164}\text{Dy}$ - $^{162}\text{Dy}$ mixture, with a quartic trap applied to $^{164}\text{Dy}$	5
24	3.3 Dipolar asymmetric $^{168}\text{Er}$ - $^{164}\text{Dy}$ mixture, with a quartic trap applied to $^{168}\text{Er}$	6
25	<b>4 Summary</b>	<b>9</b>
26	<b>References</b>	<b>9</b>

27

28

## 29 1 Dipolar Bose-Einstein condensate - Introduction

30 The experimental realization of Bose-Einstein condensation in chromium ( $^{52}\text{Cr}$ ) atoms has  
31 opened the new research direction called dipolar quantum gases [1]. Following the condensa-  
32 tion in  $^{52}\text{Cr}$ , many subsequent studies have been carried out by different experimental groups  
33 on fermionic and bosonic properties of strongly dipolar ultracold gases, such as with dyspro-  
34 sium (Dy) and erbium (Er) (see [2] and references therein). More recently, the elementary  
35 excitations spectrum of  $^{164}\text{Dy}$  and  $^{166}\text{Er}$  dipolar Bose gases were analyzed in Ref. [3], by con-  
36 sidering three-dimensional (3D) anisotropic traps across the superfluid-supersolid phase tran-  
37 sition. The recent investigations in ultracold laboratories with two-component dipolar Bose-  
38 Einstein Condensates (BEC), on stability and miscibility properties, became quite interesting  
39 due to the number of control parameters that can be explored in new experimental setups.  
40 The parameters which can be controlled are given by the strengths of dipoles, the number of  
41 atoms in each component, the inter- and intra-species scattering lengths, as well as confining  
42 trap geometries. The stability and pattern formation have been studied in Ref. [4], by consid-  
43 ering dipolar-dipolar interactions (DDIs) in two-component dipolar BEC systems. Rotational  
44 properties of two-component dipolar BEC in concentrically coupled annular traps were also  
45 studied in Ref. [5], by assuming a mixture with only one dipolar component.

46 Following previous studies with rotating binary dipolar mixtures and their miscibility prop-  
47 erties [6–8], the miscible-immiscible transition (MIT) of the dipolar mixtures with  $^{162,164}\text{Dy}$   
48 and  $^{168}\text{Er}$  were also recently studied by us in Ref. [9]. For these coupled dipolar systems,  
49 the miscible-immiscible stable conditions were analyzed within a full 3D formalism, by con-  
50 sidering repulsive contact interactions, within pancake- and cigar-type trap configurations.  
51 The rotational properties and vortex-lattice pattern structures of these dipolar mixtures were  
52 further investigated by us in Refs. [10–12], by changing the inter- to intra-species scattering  
53 lengths, as well as the polarization angles of the dipoles. Among the observed characteristics  
54 of these strong dipolar binary systems, relevant for further investigations are the possibilities  
55 to alter the effective time-averaged DDI from repulsive to attractive, by tuning the polariza-  
56 tion angle  $\varphi$  of both interacting dipoles from zero to  $90^\circ$ , respectively. In Ref. [11], vortex  
57 pattern structures were studied by considering rotating binary mixtures confined by squared  
58 optical lattices, whereas in Ref. [12], by tuning  $\varphi$ , our investigation was mainly concerned  
59 with rotational properties together with spatial separations of the binary mixtures.

60 Motivated by the above mentioned studies, considering that the interplay between DDIs  
61 and contact interactions can bring us different interesting effects in the MIT, showing richer  
62 vortex-lattice structures in rotating binary dipolar systems, in the present contribution we are  
63 also reporting some new results obtained for the properties of dipolar mixtures confined by a  
64 strongly pancake-like two-dimensional (2D) rotating harmonic trap. The effect of a weak quartic  
65 perturbation in the  $x$ - $y$  plane, applied to the first dipolar component, is studied by tuning  
66 the polarization angles of the dipoles together with the contact inter-species interactions.

67 Next section, the model formalism is presented with our parametrization and numerical  
68 procedure. In section 3, after an analysis of the main results for symmetric and asymmetric bi-  
69 nary dipolar mixtures confined by strong pancake-like harmonic traps, we present new results  
70 obtained when considering the effect of a weak quartic perturbation added to the harmonic  
71 trap of one of the components. Finally, a summary with our conclusions is given in section 4.

## 72 2 Model formalism, parametrization and numerical approach

### 73 2.1 Model formalism

74 The coupled dipolar system with condensed two atomic species  $i = 1, 2$ , with the respective  
 75 masses  $m_i$  (with  $m_1 \geq m_2$ ) are assumed to be confined in strongly pancake-shaped harmonic  
 76 traps, with fixed aspect ratios, such that  $\lambda = \omega_{i,z}/\omega_{i,\perp} = 20$  for both species  $i = 1, 2$ , where  
 77  $\omega_{i,z}$  and  $\omega_{i,\perp}$  are, respectively, the longitudinal and transverse trap frequencies. The coupled  
 78 Gross-Pitaevskii (GP) equation is cast in a dimensionless format, with energy and length units  
 79 given, respectively, by  $\hbar\omega_{1,\perp}$  and  $l_\perp \equiv \sqrt{\hbar/(m_1\omega_{1,\perp})}$ . Correspondingly, the space and time  
 80 variables are given in units of  $l_\perp$  and  $1/\omega_1$ , respectively, such that  $\mathbf{r} \rightarrow l_\perp \mathbf{r}$  and  $t \rightarrow \tau/\omega_1$ .  
 81 Within these units, and by adjusting both trap frequencies such that  $m_2\omega_{2,\perp}^2 = m_1\omega_{1,\perp}^2$ ,  
 82 the dimensionless external 3D trap potential for each one of the species  $i$  can be written as  
 83  $V_{3D,i}(\mathbf{r}) \equiv V_i(x, y) + \frac{1}{2}\lambda^2 z^2$ . On the miscibility conditions for binary trapped dipolar systems,  
 84 more details and discussion can be found in Refs. [10–12]. Large values for  $\lambda$  allow us to  
 85 reduce to 2D the original 3D formalism by considering the usual factorization of the 3D wave  
 86 function as  $\psi_i(x, y, \tau)\chi_i(z)$ , where  $\chi_i(z) \equiv (\lambda/\pi)^{1/4} e^{-\lambda z^2/2}$ . The two-body contact interac-  
 87 tions related to the scattering lengths  $a_{ij}$ , and DDI parameters are defined as [12]

$$g_{ij} \equiv \sqrt{2\pi\lambda} \frac{m_1 a_{ij} N_j}{m_{ij} l_\perp}, \quad d_{ij} = \frac{N_j \mu_0 \mu_i \mu_j}{4\pi \hbar \omega_1 l_\perp^3}, \quad a_{ii}^{(d)} \equiv \frac{1}{12\pi} \frac{m_i \mu_0 \mu_i^2}{m_1 \hbar \omega_1 l_\perp^2}, \quad a_{12}^{(d)} = a_{21}^{(d)} = \frac{1}{12\pi} \frac{\mu_0 \mu_1 \mu_2}{\hbar \omega_1 l_\perp^2}, \quad (1)$$

88 where  $i, j = 1, 2$ , with  $N_j$  being the number of atoms and  $m_{ij} = m_i m_j / (m_i + m_j)$  the reduced  
 89 mass of the species  $i$  and  $j$ . In our numerical analysis, the length unit will be assumed being  
 90  $l_\perp = 1 \mu\text{m} \approx 1.89 \times 10^4 a_0$ , with  $a_0$  being the Bohr radius. The corresponding 2D coupled GP  
 91 equation for the two components  $\psi_i \equiv \psi_i(x, y, \tau)$  of the total wave function can be written as

$$i \frac{\partial \psi_i}{\partial \tau} = \left[ \frac{-m_1}{2m_i} \nabla_{2D}^2 + V_i(x, y) - \Omega L_z + \sum_{j=1,2} g_{ij} |\psi_j|^2 + \sum_{j=1,2} d_{ij} \int dx' dy' V^{(d)}(x-x', y-y') |\psi_j'|^2 \right] \psi_i, \quad (2)$$

92 where  $\nabla_{2D}^2 \equiv \frac{\partial^2}{\partial x^2} + \frac{\partial^2}{\partial y^2}$ ,  $\psi_i' \equiv \psi_i(x', y', \tau)$ , with  $V^{(d)}(x, y)$  being the reduced 2D expression  
 93 for the DDI. The 2D confining potential  $V_i(x, y)$  is assumed to be harmonic for both compo-  
 94 nents, as in Ref. [12]. However, in the present contribution we are providing an extension to  
 95 our study reported in Ref. [12], by examining the effect, on the pattern distribution and spatial  
 96 separation of the dipolar mixture, of a quartic term applied to one of the components, which  
 97 we define as the more-massive one. So, the trap is given by

$$V_i(x, y) \equiv V_i(\rho) \equiv \frac{\rho^2}{2} + \kappa_i \rho^4, \quad \text{where } \rho \equiv \sqrt{x^2 + y^2}, \quad \kappa_2 = 0, \quad (3)$$

98 with  $\kappa_1 \equiv \kappa$  being a dimensionless positive parameter (in principle, assumed to be small),  
 99 which increases the trap confinement of the more massive component. Each component of the  
 100 wave function is assumed normalized to one,  $\int_{-\infty}^{\infty} dx dy |\psi_i|^2 = 1$ . In Eq. (2),  $L_z$  is the angular  
 101 momentum operator (in units of  $\hbar$ ), with  $\Omega$  being the corresponding rotation parameter (in  
 102 units of  $\omega_1$ ), which is assumed to be common for both components.

103 The 2D DDI presented in the integrand of the second term shown in Eq. (2) can be ex-  
 104 pressed in the 2D momentum space as the combination of two terms, by considering the  
 105 orientations of the dipoles  $\varphi$  and the projection of the corresponding Fourier transformed  
 106  $V^{(d)}(x, y)$ . One term is perpendicular, with the other parallel to the direction of the dipole  
 107 inclinations, as described in Refs. [7, 8]. By generalizing the description to a polarization field  
 108 rotating in the  $(x, y)$  plane, the two terms can be combined according to the dipole orientations  
 109  $\varphi$ , with the total 2D momentum-space DDI given by [12]

$$\tilde{V}^{(d)}(k_x, k_y) = \frac{3 \cos^2 \varphi - 1}{2} \left[ 2 - 3 \sqrt{\frac{\pi}{2\lambda}} k_\rho \exp\left(\frac{k_\rho^2}{2\lambda}\right) \text{erfc}\left(\frac{k_\rho}{\sqrt{2\lambda}}\right) \right] \equiv V_\varphi(k_\rho), \quad (4)$$

110 where  $k_\rho^2 \equiv k_x^2 + k_y^2$ , with  $\text{erfc}(x)$  being the complementary error function of  $x$ . The 2D  
 111 configuration-space effective DDI is obtained by applying the convolution theorem in Eq. (2),  
 112 performing the inverse 2D Fourier-transform for the product of the DDI and density, such that  
 113  $\int dx' dy' V^{(d)}(x-x', y-y') |\psi_j'|^2 = \mathcal{F}_{2D}^{-1} [\tilde{V}^{(d)}(k_x, k_y) \tilde{n}_j(k_x, k_y)]$ . From Eq. (4), one should  
 114 notice that such momentum-space Fourier transform of the dipole-dipole potential changes  
 115 the sign at some particular large momentum  $k_\rho$ . However, after applying the convolution  
 116 theorem with the inverse Fourier transform (by integrating the momentum variables), the  
 117 corresponding coordinate-space interaction has a definite value, as in the 3D case, which is  
 118 positive for  $\varphi \leq \varphi_M$ , and negative for  $90^\circ \geq \varphi > \varphi_M$ , where  $\varphi_M \approx 54.7^\circ$  is the so-called  
 119 “magic angle”, in which the DDI is canceled out.

## 120 2.2 Parametrization and numerical approach

121 For the two coupled dipolar systems that we are investigating, the corresponding magnetic  
 122 dipole moments of the species are the following:  $\mu = 10\mu_B$  for  $^{162,164}\text{Dy}$ , and  $\mu = 7\mu_B$  for  
 123  $^{168}\text{Er}$ . So, by considering the definitions given in (1), the strengths of the DDI are  $a_{ij}^{(d)} = 131 a_0$   
 124 ( $i, j = 1, 2$ ), for the symmetric-dipolar mixture  $^{164}\text{Dy}-^{162}\text{Dy}$ ; and  $a_{11}^{(d)} = 66 a_0$ ,  $a_{22}^{(d)} = 131 a_0$   
 125 and  $a_{12}^{(d)} = a_{21}^{(d)} = 94 a_0$ , for the  $^{168}\text{Er}-^{164}\text{Dy}$  mixture. In all the cases, we assume the number  
 126 of atoms for both species are identical and fixed at  $N_1 = N_2 = 5000$ . The number of atoms are  
 127 reduced in relation to the ones used in Ref. [12], in view of our present aim and numerical  
 128 convenience. For symmetric-dipolar mixture ( $\mu_1 = \mu_2$ ) we have  $d_{12} = d_{11} = d_{22}$ . In the case of  
 129 contact interactions, we should consider enough large repulsive scattering lengths in view of  
 130 our stability requirements. We fix both intra-species contact interactions at  $a_{11} = a_{22} = 50a_0$ ,  
 131 remaining the inter-species one to be explored by varying the ratio parameter  $\delta \equiv a_{12}/a_{11}$ .  
 132 Once selected the polarization angle and  $\delta$  as the appropriate parameters to alter the mis-  
 133 cibility properties of a mixture, we fix other parameters guided by possible realistic settings  
 134 and stability requirements. For the present approach, we choose  $\Omega = 0.75$  for the rotation  
 135 frequency parameter, larger than the one used in Ref. [12] ( $\Omega = 0.6$ ), in order to improve the  
 136 observation of vortex-pattern structures and spatial separation.

137 For the numerical approach to solve the GP formalism (2), the split-step Crank-Nicolson  
 138 method [14, 15] is applied, combined with a standard method for evaluating DDI integrals in  
 139 momentum space, as described in Ref. [12]. In the search for stable solutions, the numerical  
 140 simulations were carried out in imaginary time on a grid with a maximum of 464 points in both  
 141  $x - y$  directions, with spatial and time steps  $\Delta x = \Delta y = 0.05$  and  $\Delta t = 0.0005$ , respectively.  
 142 In this approach, both wave-function components are renormalized to one at each time step.

## 143 3 Symmetric and asymmetric dipolar mixtures - Results

### 144 3.1 Dipolar mixtures confined by identical harmonic pancake-like traps

145 We focus our study in the two coupled mixtures given by  $^{168}\text{Er}-^{164}\text{Dy}$  and  $^{164}\text{Dy}-^{162}\text{Dy}$ , moti-  
 146 vated by recent experimental studies with dipolar BEC systems. In our investigation, we have  
 147 considered harmonic strongly pancake-like trap, as detailed in Ref. [12]. First, a detailed anal-  
 148 ysis of ground state and stability properties was performed in the absence of rotation. In this  
 149 respect, we understand that our theoretical predictions can be helpful in verifying miscibility  
 150 properties in on-going experiments under different anisotropic trap configurations. The sta-  
 151 bility regime was verified for  $^{168}\text{Er}-^{164}\text{Dy}$  and  $^{164}\text{Dy}-^{162}\text{Dy}$  mixtures considering the fraction  
 152 number of atoms for each species as functions of the trap-aspect ratio  $\lambda$ . From the MIT condi-  
 153 tions for homogeneous coupled systems confined in hard-wall barriers, one can observe that

154 the miscibility remains unaffected by the dipolar interactions. In order to estimate the misci-  
 155 bility for non-homogeneous confined binary mixtures, a relevant parameter  $\eta$  was defined in  
 156 Ref. [9], by integrating the square-root of the product of the two-component densities, given by  
 157  $\eta = \int \sqrt{|\phi_1|^2 |\phi_2|^2} dx$ , which varies from  $\eta = 0$  (complete immiscible mixtures) to  $\eta = 1$  (for  
 158 complete miscible mixtures). This parameter is found appropriate for a quantitative estimate  
 159 of the overlap between the two densities of the coupled system. By considering the natural  
 160 properties of the mixed elements, the two mixtures, we notice that  $^{168}\text{Er}$ - $^{164}\text{Dy}$  and  $^{164}\text{Dy}$ -  
 161  $^{162}\text{Dy}$  have quite different miscibility behaviors, with  $^{164}\text{Dy}$ - $^{162}\text{Dy}$  being almost completely  
 162 miscible ( $\eta = 0.99$ ) and  $^{168}\text{Er}$ - $^{164}\text{Dy}$  partially miscible ( $\eta = 0.77$ ), when the other parameters  
 163 (trap-aspect ratio and number of atoms) are fixed to the same values. Such behavior is clearly  
 164 due to a mass-imbalance effect, as discussed in Ref. [12], which plays a relevant role in the  
 165 inter-species dipolar strength when compared with the intra-species one.

166 The two binary mixtures ( $^{164}\text{Dy}$ - $^{162}\text{Dy}$  and  $^{168}\text{Er}$ - $^{164}\text{Dy}$ ), respectively called “symmetric”  
 167 and “asymmetric” ones, are considered in a rotating frame within quasi 2D settings. Ow-  
 168 ing to the different miscibility properties, quite distinct vortex patterns are observed between  
 169 the symmetric and asymmetric mixtures. For the dipolar symmetric mixture,  $^{164}\text{Dy}$ - $^{162}\text{Dy}$ , we  
 170 observe the following lattice patterns: triangular, square-shaped, rectangular-shaped, double  
 171 core, striped, and with domain walls. For the dipolar asymmetric mixture,  $^{168}\text{Er}$ - $^{164}\text{Dy}$ , we no-  
 172 tice triangular, square-shaped, and circular pattern lattices. Further, to analyze the anisotropic  
 173 properties of dipolar interactions, the polarization angle  $\varphi$  of the dipoles was modified with  
 174 the dipolar interactions being tuned from repulsive to attractive. With the dipoles of the two  
 175 species polarized in the same direction, perpendicular to the direction of the dipole alignment  
 176 ( $\varphi = 0$ ), the DDI is repulsive. By tuning the polarization angle  $\varphi$  from zero to  $90^\circ$  the DDI  
 177 changes from repulsive to fully attractive, with the DDI being canceled for  $\varphi = \varphi_M \approx 54.7^\circ$ .  
 178 The miscibility of the condensed mixture is mainly affected by the inter-species interactions;  
 179 with the vortex-pattern structures being related to combined effects due to inter- and intra-  
 180 species interactions, with the vortex-pattern formations obtained with  $\varphi = 0$  surviving ap-  
 181 proximately up to  $\varphi \approx \varphi_M$ . Complete spatial separation between the two-component densi-  
 182 ties under rotation is verified for large  $\varphi$ , when the DDI is attractive. As verified, half-space  
 183 angular separations occur in dipolar-symmetric cases, represented by  $^{164}\text{Dy}$ - $^{162}\text{Dy}$ ; whereas  
 184 radial-space separations occur for dipolar-asymmetric cases, represented by  $^{168}\text{Er}$ - $^{164}\text{Dy}$ . An-  
 185 other quite relevant result obtained in Ref. [12] is the observed effect of the mass-asymmetry  
 186 in the miscibility and vortex-pattern structures. The particular mass-imbalance sensitivity can  
 187 better be appreciated in the dipolar-symmetric mixture  $^{164}\text{Dy}$ - $^{162}\text{Dy}$  for  $\delta = 1$ , when all the  
 188 differences between the density patterns should be attributed to the small mass-asymmetry.

189 Next, we report new results with the trap interaction as given by Eq. (3), with a quartic  
 190 term added to the harmonic interaction of the more-massive component of both two mixtures.

### 191 3.2 Dipolar symmetric $^{164}\text{Dy}$ - $^{162}\text{Dy}$ mixture, with a quartic trap applied to $^{164}\text{Dy}$

192 As discussed above, being dipolar symmetric, with  $a_{11} = a_{22} = 131a_0$ , this  $^{164}\text{Dy}$ - $^{162}\text{Dy}$  BEC  
 193 mixture exposes more miscible properties. As verified in Ref. [12], this mixture in the rotating  
 194 harmonic trap [with  $\kappa_i = 0$  in Eq. (3)] shows triangular, squared, rectangular-shaped, double  
 195 core, striped, and with domain wall vortex lattices regarding the ratio between inter- and  
 196 intra-species contact interaction. Also, this mixture shows complete spatial separation at large  
 197 polarization angles, where the DDI is purely attractive. By modifying the external confinement  
 198 of one of the components, we can introduce some external asymmetry to the mixture. So, in  
 199 this contribution, for this binary system we start by adding a very weak quartic term in the first  
 200 component of the mixture, in order to analyze the miscibility and complete spatial separation of  
 201 the coupled system. We consider two different miscible cases, with  $\delta = 1$  and 1.45. For these  
 202 particular cases, striped and domain wall vortex structures are observed [12], respectively,

203 when both species are under identical rotating harmonic pancake-like traps, with  $\lambda = 20$   
 204 and  $\Omega = 0.6$ . By adding a quartic term to the trap, as explained in section 2, we have also  
 205 reduced the number of atoms to  $N_i = 5000$  and increased the frequency to  $\Omega = 0.75$  in order  
 206 to improve our observation on the corresponding rotational structure and spatial separation.  
 207 In this case, ring lattice structures can be verified, also verified even for single component  
 208 BECs. From our results, in this communication, we select three different orientation angles of  
 209 the dipoles, given by  $\varphi = 0^\circ$ ,  $45^\circ$  and  $90^\circ$ , in which the first ( $\varphi = 0^\circ$ ) provides complete  
 210 repulsive DDI, the second ( $\varphi = 45^\circ$ ) is weakly repulsive, with the DDI of the third  $\varphi = 90^\circ$   
 211 being complete attractive. As shown by our results presented in Fig. 1, the small weak quartic  
 212 perturbation in the trap, given by  $\kappa = 0.05$ , induces radial spatial separations between the  
 213 condensate densities, displaying ring lattice structure in the second component as shown in  
 214 the panels (a) to (e) of Fig. 1. The quartic trap term added to the first component makes  
 215 the first component more confined than the second one. So the second component becomes  
 216 radially phase-separated, changing the previous patterns observed in Ref. [12] for  $\kappa = 0$ . Such  
 217 similar behavior for non-dipolar mixtures was also analyzed theoretically recently in Ref. [16].

218

219 To improve our understanding of the phase separation and the effect of the added quartic  
 220 trap, we studied the dipolar binary system by increasing the strength  $\kappa$ . We observed that, for  
 221  $\kappa \geq 0.1$ , with large repulsive inter-species interaction  $\delta = 1.45$ , the spatial phase separations  
 222 of the densities change completely from the previous angular to radial ones. This behavior is  
 223 indicated in Fig. 2, where the phase-separated case, displayed for  $\varphi = 90^\circ$  with  $\kappa = 0.05$ , is  
 224 being compared with the  $\kappa = 0.08$  case. So, when  $\kappa \geq 0.1$ , only radial spatial separation can  
 225 be observed in the binary mixture.

### 226 3.3 Dipolar asymmetric $^{168}\text{Er}$ - $^{164}\text{Dy}$ mixture, with a quartic trap applied to $^{168}\text{Er}$

227 In this subsection we consider the dipolar asymmetric  $^{168}\text{Er}$ - $^{164}\text{Dy}$  BEC system, to study the  
 228 effect of a quartic dipolar trap applied to the first component ( $^{168}\text{Er}$ ) of the mixture. As re-  
 229 ported in Ref. [12] for this dipolar asymmetric case, when  $\kappa_i = 0$  in the rotating confining  
 230 harmonic trap given by Eq. (3), one should observe triangular, square-shaped, and circular  
 231 lattices, by varying the inter-species interaction. The interplay between the inter-species re-  
 232 pulsive character, shown by increasing  $\delta$ , together with the attractive role of the DDI as the  
 233 polarization angle is increased, have shown radial density distributions for the binary mixture  
 234 such that for  $\varphi = 0^\circ$  and  $\delta \geq 1$  the  $^{168}\text{Er}$  element is at the center of the mixture (surrounded  
 235 by  $^{164}\text{Dy}$ ), moving to the external part when the dipolar interaction becomes more attractive,  
 236 with  $\varphi = 90^\circ$ , with an exchange of the densities.

237 Now, with the present study, by increasing the external trap interaction with the quartic  
 238 term, as given by Eq. (3) with  $\kappa = 0.05$ , one can already observe some differences in the  
 239 pattern distribution of the vortices of both mixtures, as shown in Fig. 3. However, one should  
 240 notice that, for the complete spatial separation that occurs for  $\varphi = 90^\circ$ , the position of both  
 241 elements remains as in the case that  $\kappa = 0$ , implying that the added quartic term is not enough  
 242 to change the position of the density distributions. More interesting behavior can be observed  
 243 by increasing the strength of the quartic term, as verified in the Fig. 4, by considering  $\varphi = 90^\circ$   
 244 with  $\delta = 1.45$ . In the left panels of this figure, we consider  $\kappa = 0.25$ , where we can verify  
 245 that the previous radial distribution of the densities is being modified with the radius of the  
 246 first component being reduced. With  $\kappa = 1$ , we finally obtain a radial spatial separation in  
 247 which the  $^{168}\text{Er}$  condensate is occupying the center, surrounded by the  $^{164}\text{Dy}$  condensate. The  
 248 densities of the two components interchange their positions in relation to the case that  $\kappa = 0$ ,  
 249 due to the quartic trap term, which is dominating the confinement of the  $^{168}\text{Er}$  condensate.

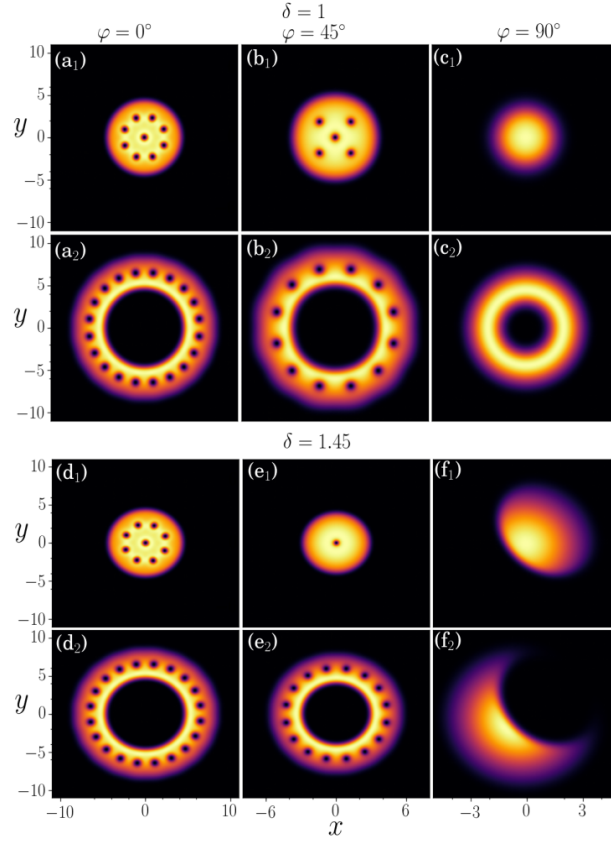


Figure 1: 2D Dipolar density patterns,  $|\psi_j|^2$ , where  $j=1$  is for  $^{164}\text{Dy}$  and  $j=2$  for  $^{162}\text{Dy}$ , are shown for  $\delta = 1$  [(a<sub>j</sub>) to (c<sub>j</sub>)] and  $\delta = 1.45$  [(d<sub>j</sub>) to (f<sub>j</sub>)]. The dipole polarization angles ( $\varphi = 0^\circ, 45^\circ, 90^\circ$ ) are indicated at the top of each column, with the  $^{164}\text{Dy}$  component having the addition of a quartic trap with  $\kappa = 0.05$ . The other parameters are:  $N_{j=1,2} = 5000$ ,  $\lambda = 20$ ,  $a_{11} = a_{22} = 50a_0$  and  $\Omega = 0.75$ .

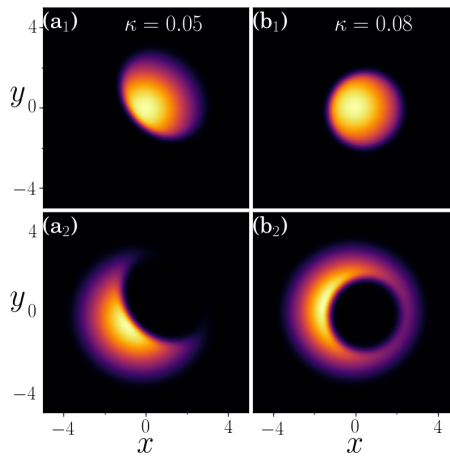


Figure 2: 2D Dipolar density patterns,  $|\psi_j|^2$ , where  $j=1$  is for  $^{164}\text{Dy}$  and  $j=2$  for  $^{162}\text{Dy}$ , are shown for  $\varphi = 90^\circ$  and  $\delta = 1.45$ . The quartic trap added to component 1 is such that  $\kappa = 0.05$  in the left panel and  $0.08$  in the right panel. As in Fig. 1, the other parameters are:  $N_{j=1,2} = 5000$ ,  $\lambda = 20$ ,  $a_{11} = a_{22} = 50a_0$  and  $\Omega = 0.75$ .

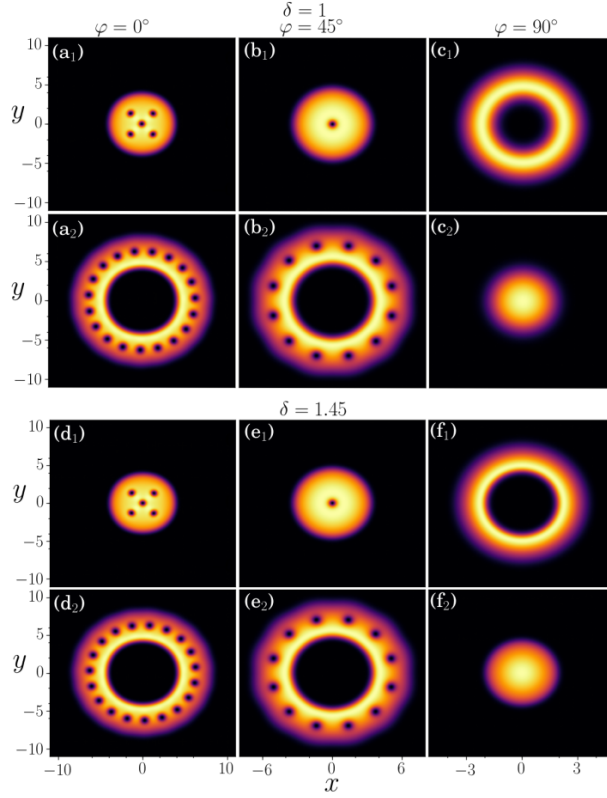


Figure 3: 2D Dipolar density patterns,  $|\psi_j|^2$ , where  $j=1$  is for  $^{168}\text{Er}$  and  $j=2$  for  $^{164}\text{Dy}$ , are shown for  $\delta = 1$  [(a<sub>j</sub>) to (c<sub>j</sub>)] and  $\delta = 1.45$  [(d<sub>j</sub>) to (f<sub>j</sub>)]. The dipole polarization angles ( $\varphi = 0^\circ, 45^\circ, 90^\circ$ ) are indicated at the top of each column, with the  $^{168}\text{Er}$  component having the addition of a quartic trap with  $\kappa = 0.05$ . The other parameters are:  $N_{j=1,2} = 5000$ ,  $\lambda = 20$ ,  $a_{11} = a_{22} = 50a_0$  and  $\Omega = 0.75$ .

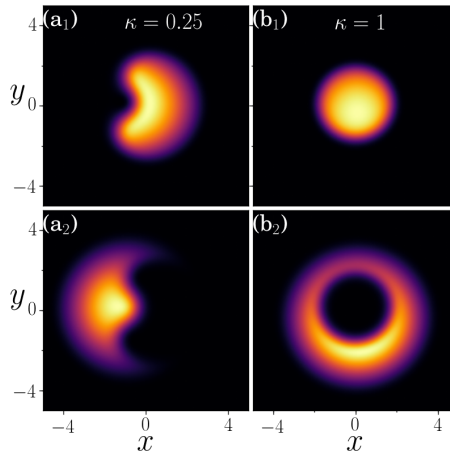


Figure 4: 2D Dipolar density patterns,  $|\psi_j|^2$ , where  $j=1$  is for  $\text{Er}-^{168}$  and  $j=2$  for  $^{164}\text{Dy}$ , are shown for  $\varphi = 90^\circ$  and  $\delta = 1.45$ . The quartic trap added to component 1 is such that  $\kappa = 0.25$  in the left panel and 1 in the right panel. As in Fig. 3, the other parameters are:  $N_{j=1,2} = 5000$ ,  $\lambda = 20$ ,  $a_{11} = a_{22} = 50a_0$  and  $\Omega = 0.75$ .



## 4 Summary

By considering the symmetric and asymmetric dipolar coupled mixtures, respectively given by  $^{164}\text{Dy}$ - $^{162}\text{Dy}$  and  $^{168}\text{Er}$ - $^{164}\text{Dy}$ , in this communication we have first discussed rotational properties, miscibility aspects, and spatial separation of these two coupled binary BEC systems, by analyzing an investigation previously reported in Ref. [12]. In addition, new results are presented by considering one of the elements of the coupled mixture being confined by a quartic interaction, which is added to the previous harmonic trap potential. The relevance of this study relies on current experimental possibilities in cold-atom laboratories to investigate such dipolar binary systems. The stability regime and miscibility properties due to the DDI of the coupled system are obtained numerically, by solving the corresponding GP equation within a model where the mixture is first confined by strong pancake-like harmonic-trap potential with aspect-ratio  $\lambda = 20$  and considering repulsive two-body interactions. The DDI are tuned from repulsive to attractive by varying the dipole polarization angle, with a clear spatial separation verified in the densities for attractive DDI, being angular for symmetric mixtures and radial for asymmetric ones in the case that no quartic term is present. In an extension of our previous reported work, by adding the quartic term to the trap interaction, here we show how the density distribution of both binary system, symmetric and asymmetric ones, are affected. As shown, the quartic trap supports radial phase separations with ring lattice for both  $^{164}\text{Dy}$ - $^{162}\text{Dy}$  and  $^{168}\text{Er}$ - $^{164}\text{Dy}$  BEC mixtures, modifying the previous vortex-pattern structures and spatial separations obtained without the quartic term interaction. Even a weak quartic trap is enough to modify the angular spatial separation to radial ones in the dipolar  $^{164}\text{Dy}$ - $^{162}\text{Dy}$  mixture, for attractive dipolar interactions. In the asymmetric  $^{168}\text{Er}$ - $^{164}\text{Dy}$  dipolar BEC mixture, where we have already radial spatial separation for attractive dipolar interactions even without the quartic term, with the  $^{168}\text{Er}$  element surrounding the other element, we have observed that, for the addition of enough large quartic term to the  $^{168}\text{Er}$  element, there is an exchange of the two coupled densities, with this element moving to the center. So, for asymmetric mixture with repulsive inter-species interaction and attractive DDI, strong quartic trap ( $\kappa \geq 1$ ) will prevent exchanges between both densities, which will remain completely radial-separated spatially.

## Acknowledgements

The authors acknowledge partial support received from Conselho Nacional de Desenvolvimento Científico e Tecnológico (CNPq) [LT, RKK and AG], Fundação de Amparo à Pesquisa do Estado de São Paulo (FAPESP) [Contracts 2016/14120-6 (LT), 2016/17612-7 (AG)]. RKK also acknowledge support from Marsden Fund (Contract UOO1726).

## References

- [1] T. Lahaye, C. Menotti, L. Santos, M. Lewenstein, T. Pfau, *The physics of dipolar bosonic quantum gases*, Rep. Prog. Phys. **72**, 126401 (2009), doi:[10.1088/0034-4885/72/12/126401](https://doi.org/10.1088/0034-4885/72/12/126401).
- [2] A. Trautmann, P. Ilzhöfer, G. Durastante, C. Politi, M. Sohmen, M. J. Mark, and F. Ferlaino, *Dipolar quantum mixtures of erbium and dysprosium atoms*, Phys. Rev. Lett. **121**, 213601 (2018), doi:[10.1103/PhysRevLett.121.213601](https://doi.org/10.1103/PhysRevLett.121.213601).
- [3] G. Natale, R.M.W. van Bijnen, A. Patscheider, D. Petter, M. J. Mark, L. Chomaz, and F. Ferlaino, *Excitation spectrum of a trapped dipolar supersolid and its experimental evidence*,

- 292 Phys. Rev. Lett. **123**, 050402 (2019), doi:[10.1103/PhysRevLett.123.050402](https://doi.org/10.1103/PhysRevLett.123.050402).
- 293 [4] K.-T. Xi, T. Byrnes, and H. Saito, H. *Fingering instabilities and pattern formation in*  
294 *a two-component dipolar Bose-Einstein condensate*, Phys. Rev. A **97**, 023625 (2018),  
295 doi:[10.1103/PhysRevA.97.023625](https://doi.org/10.1103/PhysRevA.97.023625).
- 296 [5] X. Zhang, W. Han, L. Wen, P. Zhang, R.-F. Dong, H. Chang, and S.-G. Zhang, *Two-*  
297 *component dipolar Bose-Einstein condensate in concentricly coupled annular traps*, Sci.  
298 Rep. **5**, 8684 (2015), doi:[10.1038/srep08684](https://doi.org/10.1038/srep08684).
- 299 [6] R. M. Wilson, S. Ronen and J. L. Bohn, *Stability and excitations of a dipo-*  
300 *lar Bose-Einstein condensate with a vortex*, Phys. Rev. A **79**, 013621 (2009),  
301 doi:[10.1103/PhysRevA.79.013621](https://doi.org/10.1103/PhysRevA.79.013621).
- 302 [7] R.M. Wilson, C. Ticknor, J.L. Bohn, and E. Timmermans, *Roton immiscibil-*  
303 *ity in a two-component dipolar Bose gas*, Phys. Rev. A **86**, 033606 (2012),  
304 doi:[10.1103/PhysRevA.86.033606](https://doi.org/10.1103/PhysRevA.86.033606).
- 305 [8] X.F. Zhang, L. Wen, C.-Q. Dai, R.-F. Dong, H.-F. Jiang, H. Chang, and S.-G. Zhang, *Exotic*  
306 *vortex lattices in a rotating binary dipolar Bose-Einstein condensate*, Sci. Rep. **6**, 19380  
307 (2016), doi:[10.1038/srep19380](https://doi.org/10.1038/srep19380).
- 308 [9] R.K. Kumar, P. Muruganandam, L. Tomio, and A. Gammal, *Miscibility in coupled dipo-*  
309 *lar and non-dipolar Bose-Einstein condensates*, J. Phys. Commun. **1**, 035012 (2017),  
310 doi:[10.1088/2399-6528/aa8db5](https://doi.org/10.1088/2399-6528/aa8db5).
- 311 [10] R.K. Kumar, L. Tomio, B.A. Malomed and A. Gammal, *Vortex lattices in binary Bose-*  
312 *Einstein condensates with dipole-dipole interactions*, Phys. Rev. A **96**, 063624 (2017),  
313 doi:[10.1103/PhysRevA.96.063624](https://doi.org/10.1103/PhysRevA.96.063624).
- 314 [11] *Vortex patterns in rotating dipolar Bose-Einstein condensate mixtures with squared optical*  
315 *lattices*. J. Phys. B **52**, 025302 (2018), doi:[10.1088/1361-6455/aaf332](https://doi.org/10.1088/1361-6455/aaf332).
- 316 [12] R.K. Kumar, L. Tomio and A. Gammal, *Spatial separation of rotating binary Bose-*  
317 *Einstein condensates by tuning the dipolar interactions*, Phys. Rev. A **99**, 043606 (2019),  
318 doi:[10.1103/PhysRevA.99.043606](https://doi.org/10.1103/PhysRevA.99.043606).
- 319 [13] S. Giovanazzi, A. Görlitz, and T. Pfau, *Tuning the dipolar interaction in quantum gases*,  
320 Phys. Rev. Lett. **89**, 130401 (2002), doi:[10.1103/PhysRevLett.89.130401](https://doi.org/10.1103/PhysRevLett.89.130401).
- 321 [14] R.K. Kumar, et al., *Fortran and C programs for the time-dependent dipolar Gross-*  
322 *Pitaevskii equation in an anisotropic trap*, Comput. Phys. Commun. **195**, 117-128 (2015),  
323 doi:[10.1016/j.cpc.2015.03.024](https://doi.org/10.1016/j.cpc.2015.03.024);
- 324 [15] R.K. Kumar, et al., *C and Fortran OpenMP programs for rotating Bose-Einstein condensates*,  
325 Comput. Phys. Commun. **240**, 74-82 (2019), doi:[10.1016/j.cpc.2019.03.004](https://doi.org/10.1016/j.cpc.2019.03.004).
- 326 [16] S.K. Adhikari, *Phase-separated vortex-lattice in a rotating binary Bose-Einstein*  
327 *condensate*, Commun. Nonlinear Sci. Numer. Simul. **71**, 212 (2019),  
328 doi:[10.1016/j.cnsns.2018.11.019](https://doi.org/10.1016/j.cnsns.2018.11.019).